を施行し，年齢，性別，教育年数を考慮した上で認知の各要素での平均値，標準偏差を算出し，この結果からノーマル群，Pre-Dementia-1SD (PD-1SD) 群，Pre-Dementia-1.5SD (PD-1.5SD) 群の 3 群を設定した．ノーマルとは，5 問題すべてにおいて得点が平均値マイナス 1SD より上である状態とした．PD-1SD は，記憶はマイナス 1SD 以下であり，他は 1SD 以内にある状態とした．また，PD-1.5SD とは，記憶のみ 1.5SD 以上低下し，他は 1SD 以内にある状態とした．この結果に基づき，ノーマル群 91 名（男 43/女 48, 平均年齢±SD 72.7±5.0 歳), PD-1SD 群 33 名 (18/15, 72.6±5.1), PD-1.5SD 群 19 名 (9/10, 72.2±5.6) に分類し，これらの対象に MRI 3D-T1 強調画像および ^{99m}Tc-ECD による SPECT の撮像を施行した．なお，各群間で年齢，男女比に有意差は認められなかった．

頭部 MRI 撮像

1.5T MRI scanner (Symphony, Siemens, Erlangen, Germany) を用い，MPRAGE 法にて，前交連と後交連の中心を通る線に垂直な矢状断連続スライスを得る 3 次元 T1 強調画像の撮像を行った．条件は TE/TR 3.93/2,800 ms, flip angle 12 deg, field of view 280 mm, acquisition matrix 512×512, slice thickness 1.20 mm, Gapless とした．

SPECT データ収集・処理方法

SPECT 装置には PHILIPS 社製 3 検出器型ガンマカメラ PRISM IRIX, 画像処理装置には PICKER 社製 ODYSSEY FX を用い，コリメータには低エネルギー高分解能パラレルコリメータを使用した．収集条件は，安静閉眼にて ^{99m}Tc-ECD 740 MBq を定速静注し，10 分後から 15 分間 128×128 マトリックスの投影データを 1 ステップ 30 秒，1 カメラにつき 30 方向収集した．画像再構成は ramp filter によるフィルター逆投影法(FBP)で行い，後処理には low pass filter (cutoff : 0.71 cycle/cm, order : 8.0, 2.2 mm/pixel) を用いた．吸収補正は Chang 法を用い輪郭抽出で行った．SPECT 画像のスライス厚は 2.2 mm とした．

画像処理

MRI

得られた MRI 画像は，UNIX Workstation (Sun SPARC Solaris) 上で ANALYZE version 2.5 (Biological Imaging Resource, Mayo Foundation, Rochester, Minn.) を用いて 3 次元方向に等しい大きさとし，矢状断像から横断像を再構成した．

部分容積 (PVE) 効果補正

SPECT の低解像度に由来する部分容積効果を補正するために Matsuda ら (Matsuda et al., 2003) の方法にもとづいて PVE 補正を行った．補正方法の要旨は以下の通りである．まず，MRI と SPECT 画像を重ね合わせた．次に MRI 画像を灰白質と白質に分離し，この白質像の信号値の 95% を閾値とすることにより自動的に白質の関心領域 (ROI) を SPECT 像に設定した．この白質の SPECT 値を MRI から求めた白質像に乗じた後，MRI と重ね合わせをした SPECT 画像から差し引いた．これにより，灰白質の SPECT 像が得られ，最後に灰白質の SPECT 像を灰白質の MRI 像で除することにより PVE が補正された灰白質の SPECT 像を得た．この一連の流れを自動化したソフトウェア (Kanetaka et al., 2004) を用いて対象者の全 SPECT 画像の部分容積効果補正を行った．

画像統計解析

まず，視察法により，MRI 上明らかな梗塞巣や出血性病変のあるものは解析より除外した．画像統計解析は Matlab 5.3 for Windows

(Mathworks Inc.) 上で作動するSPM99 (www.fil.ion.ucl.ac.uk/spm/) を用いて行った. 脳萎縮の影響を考慮するために, SPECTでの群間比較に加えて, MRIより抽出した脳灰白質像を用いたvoxel based morphometry (VBM) (Ashburner and Friston, 2000) における群間比較も行った. 従来の同様の研究ではこのような補正がなされていないので, アーティファクトをみてきた可能性も否定できない. 部分容積効果補正前後でのSPECT像, MRI脳灰白質像は各々SPM99を用いて線形変換と非線形変換により標準脳に合わせ込まれた. さらに, Gaussianカーネルを用いて平滑化を行った. これらの操作により, 仮説に基づくことなく, 全脳領域の画像のボクセル単位での統計検定が可能となった. その後, ノーマル群とamnestic AACD群, amnestic MCI群で各々2群間のt検定を行った.

Table 1. Regions and peaks of significant decrease in rCBF after correction for partial volume effects (t-test, $p<0.01$, uncorrected for multiple comparison, ext 50)

Region	BA	K	t-value	coordinate x	Y	z
PD-1SD < Normal						
R Precentral gyrus	BA6	303	3.72	48	−4	30
L Precuneus	BA7	276	3.25	−14	−56	43
L Middle frontal gyrus	BA6	166	3.07	−16	4	46
PD-1.5SD < Normal						
R Middle temporal gyrus	BA19, 39	1,125	3.63	26	−86	26
R Precentral gyrus	BA6	286	3.45	50	−10	28
R Inferior frontal gyrus	BA47	331	3.26	34	35	2
R Precuneus	BA7	135	3.14	24	−58	43
R Inferior temporal gyrus	BA20	60	2.71	40	−18	−16
L Postcentral gyrus	BA47	50	2.60	−51	−16	28
PD-1.5SD < PD-1SD						
R Precentral Gyrus	BA 44	364	3.38	48	8	11
R Middle Temporal Gyrus	BA 19, 40	1,069	3.26	42	−79	19
R Supramarginal Gyrus	BA 40		3.22	59	−47	23
L Middle Temporal Gyrus	BA 21	169	3.11	−50	−1	−13
R Parahippocampal Gyrus	BA 35, 36	648	2.51	26	−15	−24
R Middle Frontal Gyrus	BA 10	253	3.00	32	49	18
L Precuneus	BA 7	148	2.88	−10	−74	37
L Parahippocampal Gyrus	BA 35, 30	428	2.85	−22	−25	−24
R Medial Frontal Gyrus	BA 10	104	2.59	6	48	−6

BA : Brodmann's area PD : Pre-Dementia
Note. Results are listed by clusters and in decreasing order of peak t-value. Cluster size is indicated by the value K, which represents the number of significant voxels in the particular cluster. Coordinates were according to the atlas by Talairach and Tournoux (Talairach and Tournoux, 1988).

結　果

1. PVE補正後SPECT画像

SPM99を用いた，ノーマルとPD-1SD，PD-1.5SDのグループ解析の結果をFig. 1ならびにTable 1に示す．PD-1SDではノーマルに比し，左楔前部，右運動前野，左中前頭回に血流低下が認められた（Fig. 1-A）．PD-1.5SDでは右楔前部，右運動前野に加えて右海馬領域にて血流低下が認められた（B）．PD-1SDとPD-1.5SDの群間比較においては，PD-1.5SDはPD-1SDと比較して左楔前部，両側海馬傍回において有意な血流低下を呈していた（C）．

2. VBM

Fig. 2とTable 2にVBMによる群間比較の結果を示す．PD-1SDではノーマルと比較して右下頭頂小葉，右楔前部，左尾状核に灰白質密度の低下を認めた(Fig. 2-A)．PD-1.5SDでは，左中側頭回，右海馬傍回にて有意な灰白質密度の低下を認めた（B）．PD-1SDとPD-1.5SDの群間比較においてはPD-1.5SDで両側海馬傍回において有意な灰白質密度の低下を認めた（C）．

考　察

従来のMCI画像研究の報告では，画像解析対象者は，記憶障害を主訴として専門医療機関を受診した群である．こうした人々は，痴呆ではなく軽度認知機能障害と診断されてはいても，実は記憶障害が明らかなことが多い．今回，我々は心理検査を施行した1,711人の結果から年齢，性，教育年数を考慮した平均値，標準偏差を求めて平均より1SD，1.5SD以上低い対象者を操作的にPD-1SD，PD-1.5SDと区分した．従来の報告では24点前後をカットオフとしたものが多いが，本研究の対象者におけるMini Mental State Examination（MMSE）の得点はほぼ全例で27点以上であった．このように，記憶障害を含めた認知機能の障害が無いかあっても非常に軽微な集団を対象とした点に本研究の1つの特徴がある．

次に先行報告（Kogure et al., 2000, Ohnishi et al., 2001）におけるノーマルデータベース作

Table 2. Regions and peaks of significant decrease in Gray Matter Density (t-test, $p<0.01$, uncorrected for multiple comparison, ext 100)

Region	BA	K	t-value	coordinate x	Y	z
PD-1SD＜Normal						
R Inferior parietal lobule	BA40	149	3.37	38	−43	39
R Precuneus	BA7	184	2.91	20	−52	50
L Caudate tail		122	2.79	−34	−29	−4
PD-1.5SD＜Normal						
L Middle temporal gyrus	BA19, 37	870	3.56	−44	−81	19
R Parahippocampal gyrus	BA20	219	3.06	18	−35	−3
L Uncus	BA28	310	2.85	−28	5	−20
PD-1.5SD＜PD-1SD						
R Parahippocampal gyrus	BA35, 36	759	3.96	26	−27	−27
L Parahippocampal gyrus	BA35, 36	199	3.13	−20	−25	−24

Note. See footnote of Table 1.

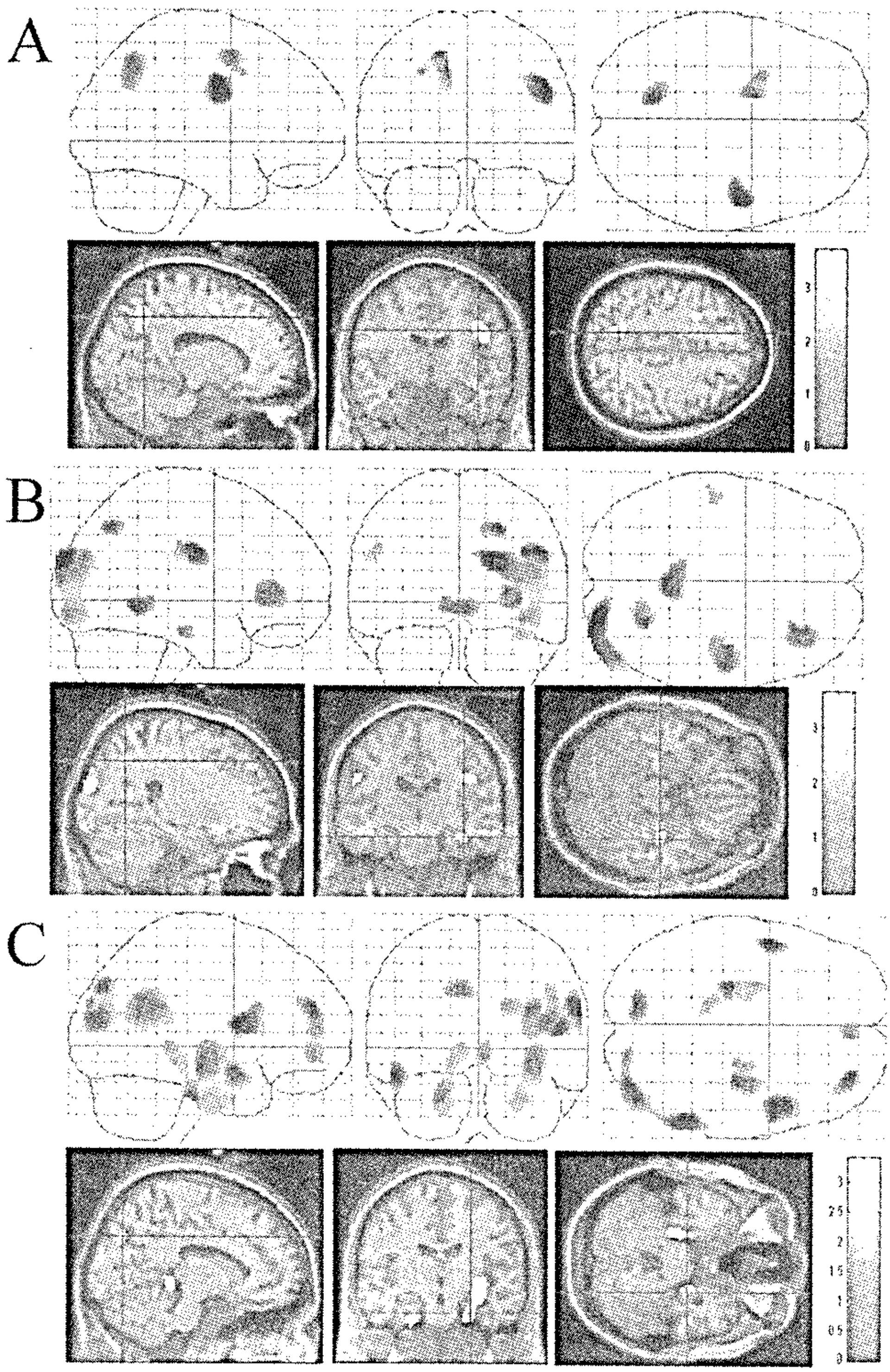

Fig. 1 Significant reduction of regional cerebral blood flow after PVE correction
A : Pre-dementia-1SD (PD-1SD) showed reduced perfusion in lt. precuneus and rt. premotor compared to normal. B : Pre-dementia-1.5SD (PD-1.5SD) showed reduced perfusion in the rt. hippocampal region in addition to the rt. precuneus and rt. premotor compared to normal. C : PD-1.5SD showed significant hypoperfusion in lt. precuneus and the bilateral parahippocampal gyri compared to PD-1SD. ($p<0.01$, uncorrected for multiple comparison, extent 50)

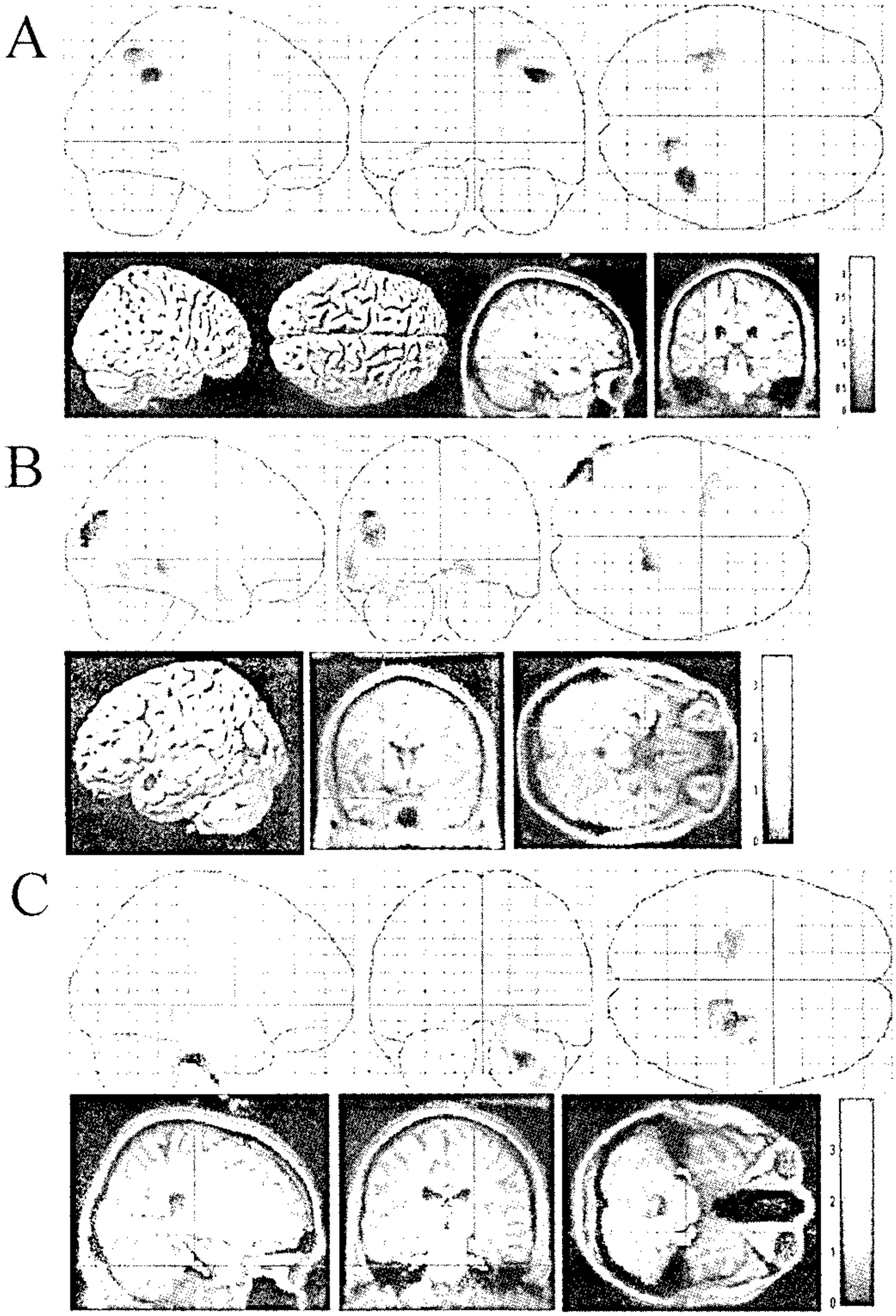

Fig. 2　Significant reduction of regional gray matter density
A : PD-1SD showed reduction in rt. inferior parietal lobule and rt precuneus compared to normal.　B : PD-1.5SD showed reduction in lt. middle temporal lobe and rt. parahippocampal gyrus compared to normal.　C : PD-1.5SD showed significant reduction in the bilateral parahippocampal gyri compared to PD-1SD. ($p<0.01$, uncorrected for multiple comparison, extent 100)

成の構成員すなわち対照は，知的に健常な人々とはいっても，生活水準や環境などの要因は様々に異なっている．しかし今回の健常対照は同一の地域に住んでおり，生活水準も比較的類似していると思われる点にも本研究の特徴がある．

これまでに，早期アルツハイマー病においては帯状回後部および楔前部での血流や代謝が低下することが指摘されてきた（Minoshima et al., 1994, Matsuda, 2001, Nestor et al., 2003）．しかし今回の我々の結果ではPD-1SDとPD-1.5SDにおいて帯状回後部での血流低下は認められず，楔前部においてのみ血流低下が認められた．この所見からは，従来，帯状回後部，楔前部と一括されていた初期ADの血流障害は楔前部から始まり，帯状回後部に広がっていくものと推測できる．

神経心理学的な機能との照合に注目すると，fMRIやPETによる賦活試験の結果から，楔前部がエピソード記憶の再生に関与しているという報告がなされている（Lundstrom et al., 2003, Backman et al., 1999, Krause et al., 1999）．また，楔前部と帯状回後部の機能の差異に関して，McDermottらは，帯状回後部がエピソード記憶の符号化においてより賦活されるのに対して，楔前部はエピソード記憶の再生でより賦活されたと報告している（McDermott et al., 1999）．我々が記憶検査として採用したバッテリーはcategory cued recallであるところから，楔前部の血流低下はエピソード記憶の再生と近縁の機能障害をとらえている可能性が考えられる．これに関係するのがPD-1SD, PD-1.5SDともに右運動前野に血流低下を認めたという予想外の結果である．運動前野は随意運動の選択，計画，実行を司る部位として知られてきた．近年の記憶のシステム回路研究において，運動前野はワーキングメモリーに加えて広義のエピソード記憶に属する手がかり再生と再認のネットワークの構成要素になっていることが明らかにされている（Nyberg et al., 2002）．したがって右運動前野の血流低下がcategory cued recall課題の低得点を反映しているという結果は納得できるものである．もっとも，PD-1SDやPD-1.5SDは複数の異なる症候群であるところからいわばアーティファクトとしてこの所見が得られた可能性も否定できない．

次にPD-1SDとPD-1.5SDの群間比較により，PD-1.5SDにて両側海馬傍回，左楔前部に有意な血流低下を認めた．早期ADのSPECTでは海馬領域での血流低下は認められないと考えられていたが，Matsudaらは PVE補正をすることにより，早期ADでも海馬傍回の血流低下が認められることを報告している（Matsuda et al., 2002）．VBMの結果としてPD-1SDでは右下頭頂小葉に軽度の萎縮を認めただけであったのに対して，PD-1.5SDでは右海馬傍回ならびに両側海馬傍回で灰白質の有意な萎縮を認めた．OhnishiらはVBMにてADでは海馬領域，特に嗅内野での萎縮があることを報告している（Ohnishi et al., 2001）．このようにPD-1SDとPD-1.5SDの基本的パターンは類似しているが，PD-1.5SDでは海馬傍回において血流が低下し，形態的にも萎縮を呈していた．このことから，PD-1SDとPD-1.5SDには連続性があること，また前者はより病的変化が進行した状態であること，すなわちPD-1.5SDとは既にADの極早期である可能性が考えられる．

我々は今回の対象者の脳機能画像および脳形態画像の変化を1年ごとに追跡している．そのデータからPD-1SD, PD-1.5SDのADへの移行率，そしてADに移行していくケースの予測因子を評価していくことが今後の課題である．

文　献

1. Ashburner J and Friston KJ (2000) Voxel-based morphometry—the methods. Neuroimage, 11, 805-21.
2. Backman L, Andersson JL, Nyberg L, Winblad B, Nordberg A and Almkvist O (1999) Brain regions associated with episodic retrieval in nor-

mal aging and Alzheimer's disease. Neurology, 52, 1861-70.
3. Grober E, Buschke H, Crystal H, Bang S and Dresner R (1988) Screening for dementia by memory testing. Neurology, 38, 900-3.
4. Huang C, Wahlund LO, Svensson L, Winblad B and Julin P (2002) Cingulate cortex hypoperfusion predicts Alzheimer's disease in mild cognitive impairment. BMC Neurol, 2, 9.
5. Kanetaka H, Matsuda H, Asada T, Ohnishi T, Yamashita F, Imabayashi E, Tanaka F, Nakano S, Takasaki M (2004) Effects of partial volume correction on discrimination between very early Alzheimer's dementia and controls using brain perfusion SPECT. Eur J Nucl Med Mol Imaging, 31: 975-80.
6. Kogure D, Matsuda H, Ohnishi T, Asada T, Uno M, Kunihiro T, Nakano S and Takasaki M (2000) Longitudinal evaluation of early Alzheimer's disease using brain perfusion SPECT. J Nucl Med, 41, 1155-62.
7. Krause BJ, Schmidt D, Mottaghy FM, Taylor J, Halsband U, Herzog H, Tellmann L and Muller-Gartner HW (1999) Episodic retrieval activates the precuneus irrespective of the imagery content of word pair associates. A PET study. Brain, 122 (Pt 2), 255-63.
8. Levy R (1994) Aging-associated cognitive decline. Working Party of the International Psychogeriatric Association in collaboration with the World Health Organization. Int Psychogeriatr, 6, 63-8.
9. Lundstrom BN, Petersson KM, Andersson J, Johansson M, Fransson P and Ingvar M (2003) Isolating the retrieval of imagined pictures during episodic memory: activation of the left precuneus and left prefrontal cortex. Neuroimage, 20, 1934-43.
10. Matsuda H (2001) Cerebral blood flow and metabolic abnormalities in Alzheimer's disease. Ann Nucl Med, 15, 85-92.
11. Matsuda H, Kanetaka H, Ohnishi T, Asada T, Imabayashi E, Nakano S, Katoh A and Tanaka F (2002) Brain SPET abnormalities in Alzheimer's disease before and after atrophy correction. Eur J Nucl Med Mol Imaging, 29, 1502-5.
12. Matsuda H, Ohnishi T, Asada T, Li ZJ, Kanetaka H, Imabayashi E, Tanaka F and Nakano S (2003) Correction for partial-volume effects on brain perfusion SPECT in healthy men. J Nucl Med, 44, 1243-52.
13. McDermott KB, Ojemann JG, Petersen SE, Ollinger JM, Snyder AZ, Akbudak E, Conturo TE and Raichle ME (1999) Direct comparison of episodic encoding and retrieval of words: an event-related fMRI study. Memory, 7, 661-78.
14. Mendez AMF, (2000) Cognitive function, mood, and behavior assessments, In: Comprehensive geriatric assessment. (Osterweil D, Brummel-Smith K, Beck JC, ed) pp67-119, McGraw-Hill, New York
15. Minoshima S, Foster NL and Kuhl DE (1994) Posterior cingulate cortex in Alzheimer's disease. Lancet, 344, 895.
16. Minoshima S, Giordani B, Berent S, Frey KA, Foster NL and Kuhl DE (1997) Metabolic reduction in the posterior cingulate cortex in very early Alzheimer's disease. Ann Neurol, 42, 85-94.
17. Monsch AU, Bondi MW, Butters N, Salmon DP, Katzman R and Thal LJ (1992) Comparisons of verbal fluency tasks in the detection of dementia of the Alzheimer type. Arch Neurol, 49, 1253-8.
18. Nestor PJ, Fryer TD, Ikeda M and Hodges JR (2003) Retrosplenial cortex (BA 29/30) hypometabolism in mild cognitive impairment (prodromal Alzheimer's disease). Eur J Neurosci, 18, 2663-7.
19. Nyberg L, Forkstam C, Petersson KM, Cabeza R and Ingvar M (2002) Brain imaging of human memory systems: between-systems similarities and within-system differences. Brain Res Cogn Brain Res, 13, 281-92.
20. Ohnishi T, Matsuda H, Tabira T, Asada T and Uno M (2001) Changes in brain morphology in Alzheimer disease and normal aging: is Alzheimer disease an exaggerated aging process? Am J Neuroradiol, 22, 1680-5.
21. Petersen RC, Doody R, Kurz A, Mohs RC, Morris JC, Rabins PV, Ritchie K, Rossor M, Thal L and Winblad B (2001) Current concepts in mild cognitive impairment. Arch Neurol, 58, 1985-92.
22. Petersen RC, Smith GE, Waring SC, Ivnik RJ, Tangalos EG and Kokmen E (1999) Mild cognitive impairment: clinical characterization and outcome. Arch Neurol, 56, 303-8.
23. Ritchie K, Artero S and Touchon J (2001) Classification criteria for mild cognitive impairment: a population-based validation study. Neurology, 56, 37-42.
24. Sohlberg MM and Mateer CA (1986) Attention Process Training Association for Neuropsychological Research and Development, Wasington
25. Stern CE, Owen AM, Tracey I, Look RB, Rosen BR and Petrides M (2000) Activity in ventrolateral and mid-dorsolateral prefrontal cortex during nonspatial visual working memory

processing: evidence from functional magnetic resonance imaging. Neuroimage, 11, 392-9.
26. Talairach, J., and Tournoux, P. (1988) Co-planar Stereotactic Atlas of the Human Brain. 3-Dimensional Proportional System: An Approach to Cerebral Imaging. Thieme, New York.
27. Wechsler D (1981) WAIS-R manual The Psychological Corporation, New York
28. Wolf H, Jelic V, Gertz HJ, Nordberg A, Julin P and Wahlund LO (2003) A critical discussion of the role of neuroimaging in mild cognitive impairment. Acta Neurol Scand Suppl, 179, 52-76.

Regional cerebral blood flow change and gray matter loss in mild cognitive impairment : a community-based study

Kiyotaka Nemoto[1)3)], Fumio Yamashita[2)], Takashi Ohnishi[3)], Etsuko Imabayashi[3)], Kentaro Hirao[3)], Hiromu Yokozeni[2)], Megumi Sasaki[2)], Katsuyoshi Mizukami[2)], Hiroshi Matsuda[4)], and Takashi Asada[2)]

[1)]Division of Psychiatry, Tsukuba University Hospital (2-1-1 Amakubo Tsukuba, Ibaraki 305-8576 Japan)

[2)]Department of Psychiatry, Institute of Clinical Medicine, University of Tsukuba (1-1-1 Tennodai Tsukuba, Ibaraki 305-8577 Japan)

[3)]Department of Radiology, National Center Hospital of Mental, Nervous, and Muscular Disorders, National Center of Neurology and Psychiatry (4-1-1 Ogawahigashi Kodaira, Tokyo 187-8551 Japan)

[4)]Department of Nuclear Medicine, Saitama Medical School Hospital (38 Morohongo Moroyama Iruma, Saitama 350-0495 Japan)

In this study we investigated the abnormalities of cerebral blood flow and cortical atrophy of pre-dementia subjects in a community using Tc-99m ECD SPECT and structural MRI. First, a neuropsychological test battery was administered to 1711 community-dwelling individuals aged 65 years and older. Three groups of participants, namely normal, Pre-Dementia-1SD (PD-1SD), and PD-1.5SD according to the mean value and SD gained from the test participated in the study. Thirty-three PD-1SD, 19 PD-1.5SD, and 91 normal subjects underwent both whole brain structural MRI and Tc-99m ECD SPECT. SPECT images were corrected for partial volume effects (PVEs). Using SPM99, voxel based group comparisons were made on the PVEs corrected SPECT images and voxel based morphometry (VBM) was applied to gray matter extracted from MRI images. Hypoperfusion in precuneus and right premotor cortex is found in both PD-1SD and PD-1.5SD. In addition, the PD-1.5SD individuals showed hypoperfusion in parahippocampal gyrus. VBM showed hippocampal atrophy in the PD-1.5SD individuals. These findings suggest that PD-1.5SD indicates the very early stage of AD, and the PD-1SD appears to precede the PD-1.5SD.

Address correspondence to Dr. Takashi Asada, Department of Psychiatry, Institute of Clinical Medicine, University of Tsukuba, 1-1-1 Tennodai Tsukuba, Ibaraki 305-8577, Japan

THE JOURNAL OF BIOLOGICAL CHEMISTRY
Vol. 279, No. 17, Issue of April 23, pp. 17587–17595, 2004
Printed in U.S.A.

The Effect of Cholesterol and Monosialoganglioside (GM1) on the Release and Aggregation of Amyloid β-Peptide from Liposomes Prepared from Brain Membrane-like Lipids*

Received for publication, August 5, 2003, and in revised form, December 31, 2003
Published, JBC Papers in Press, January 6, 2004, DOI 10.1074/jbc.M308622200

Yoshihiko Tashima‡, Ryoko Oe‡, Sannamu Lee‡§, Gohsuke Sugihara‡, Eric J. Chambers¶, Mitsuo Takahashi‖, and Tatsuo Yamada**

*From the ‡Department of Chemistry, Faculty of Science, the ‖Faculty of Pharmaceutical Sciences, and the **School of Medicine, Fukuoka University, Fukuoka 814-0180, Japan and the ¶Department of Pharmaceutical Sciences, University of Southern California, Los Angeles, California 90089-9121*

In order to investigate the influence of cholesterol (Ch) and monosialoganglioside (GM1) on the release and subsequent deposition/aggregation of amyloid β peptide (Aβ)-(1–40) and Aβ-(1–42), we have examined Aβ peptide model membrane interactions by circular dichroism, turbidity measurements, and transmission electron microscopy (TEM). Model liposomes containing Aβ peptide and a lipid mixture composition similar to that found in the cerebral cortex membranes (CCM-lipid) have been prepared. In all, four Aβ-containing liposomes were investigated: CCM-lipid; liposomes with no GM1 (GM1-free lipid); those with no cholesterol (Ch-free lipid); liposomes with neither cholesterol nor GM1 (Ch-GM1-free lipid). In CCM liposomes, Aβ was rapidly released from membranes to form a well defined fibril structure. However, for the GM1-free lipid, Aβ was first released to yield a fibril structure about the membrane surface, then the membrane became disrupted resulting in the formation of small vesicles. In Ch-free lipid, a fibril structure with a phospholipid membrane-like shadow formed, but this differed from the well defined fibril structure seen for CCM-lipid. In Ch-GM1-free lipid, no fibril structure formed, possibly because of membrane solubilization by Aβ. The absence of fibril structure was noted at physiological extracellular pH (7.4) and also at liposomal/endosomal pH (5.5). Our results suggest a possible role for both Ch and GM1 in the membrane release of Aβ from brain lipid bilayers.

The pathology of Alzheimer's disease (AD)[1] includes extracellular amyloid plaques, intraneuronal neurofibrillary tangles, synaptic loss, and neuronal cell death. The major components of amyloid plaques are the amphiphilic 40 and 42 residue peptides, Aβ-(1–40) and Aβ-(1–42) (1, 2). Amyloid β-peptide (Aβ) consists of a hydrophilic N-terminal region (residues 1–28) and a hydrophobic C-terminal region (residues 29–40 or 29–42). The hydrophobic part of Aβ is originally part of a transmembrane α-helix of APP anchored in the membrane of several subcellular compartments, including the ER (3). Proteolysis by the enzyme(s) γ-secretase leads to the formation of Aβ within the membrane. Thus, the membrane release of Aβ following this enzyme cleavage should play a pivotal role in subsequent amyloid plaque formation.

Recent studies have shown that the interaction of Aβ and lipids plays an important role in the pathogenesis of AD. For instance, the fibrillogenic properties of Aβ are in part a consequence of the composition of the membrane in which it resides, its peptide sequence, and its mode of assembly within the membrane (4). In terms of membrane composition, Ch and GM1 in neuronal cell membranes are widely accepted to be modulators of membrane-associated Aβ fibrillogenesis and neurotoxicity (5, 6). The formation of GM1-bound Aβ, which is thought to be a seed for the formation of toxic amyloid fiber, depends on the concentration of Ch in model membranes prepared from GM1/Ch/sphingomyelin (SM) (7). Additionally, oligomeric Aβ can promote the release of lipids from asterocytes and neurons by forming Aβ-lipid particles consisting of Ch, phospholipids, and GM1 (8).

It has been suggested that Aβ-(1–42) is essential to the early development of AD pathology but is not alone sufficient to promote the formation of mature neuritic plaques unless it is succeeded by the deposition of Aβ-(1–40) (9). Compared with Aβ-(1–40), Aβ-(1–42) has been shown to have a greater potential for aggregation (10). Studies of Aβ-lipid interaction using total brain lipid extract have shown that the peptides interact in different ways: 1) Aβ-(1–40) destabilizes model membranes and 2) Aβ-(1–42) initially destabilizes but then with time proceeds to stabilize the membrane (11). These findings are consistent with a "seeding" hypothesis, in which the aggregates of Aβ-(1–42) act as an initiation factor for early plaque formation, which is then followed by the progressive accumulation of Aβ-(1–40) in the AD brain. So too, they provide an insight into a mechanism of fibrillogenesis, which is at least in part controlled by the release of Aβ from the membrane.

AD is a disease that involves attack of the central cerebral cortex. To investigate how Ch and the ganglioside GM1 may influence the release of Aβ-(1–40) and Aβ-(1–42) from cerebral cortex membranes we have prepared and examined some model Aβ-containing liposomes. The liposomes are composed of a lipid-mixture similar in composition to cerebral cortex membranes (CCM-lipid). The liposomes prepared were of four different lipid compositions (see Table I); CCM-lipid, liposomes with no GM1 (GM1-free lipid), liposomes without cholesterol (Ch-free lipid), and liposomes without GM1 and Ch (Ch-GM1-

* The costs of publication of this article were defrayed in part by the payment of page charges. This article must therefore be hereby marked "*advertisement*" in accordance with 18 U.S.C. Section 1734 solely to indicate this fact.

§ To whom correspondence should be addressed. Tel.: 81-92-871-6631 (ext. 6248); Fax: 81-92-865-6030; E-mail: leesan@cis.fukuoka-u.ac.jp.

[1] The abbreviations used are: AD, Alzheimer's disease; Aβ, amyloid β-peptide; APP, amyloid precursor protein; CCM-lipid, a lipid-mixture similar to the composition of cerebral cortex membrane; Cer, galactocerebroside; Ch, cholesterol; CD, circular dichroism; Me_2SO, dimethylsulfoxide; egg PC, egg yolk L-α-phosphatidylcholine; egg PE, egg yolk L-α-phosphatidylethanolamine; GM1, monosialoganglioside GM1; HFIP, 1,1,1,3,3,3-hexafluoro-2-propanol; PS, L-α-phosphatidyl-L-serine; SM, sphingomyelin; TEM, transmission electron microscopy.

TABLE I
Composition of lipids in the peptide-containing liposomes of this study

	Cerebral cortex lipid[a]	CCM-lipid	Ch-free lipid	GM1-free lipid	Ch-GM1-free lipid
	w/w %	*mol %*			
PC	13.9	15.4 (14.0)	18.8	17.1	20.4
PS	8.0	8.9 (7.0)	13.3	9.8	11.7
PE	23.9	26.5 (24.0)	29.2	29.4	31.4
SM	8.0	8.9 (4.0)	12.5	9.8	11.7
Ch	13.3	14.8 (26.0)		16.3	
Cerebroside	14.3	15.9 (15.0)	16.6	17.6	21.0
GM1	8.75	9.7 (4.0)	9.6		
Plasmalogen	9.94				

[a] Values for CCM-lipid are those of Rossiter (Ref. 24).

free lipid). Liposomes were prepared by hydrating an organic film composed of a mixture of Aβ and one of the four lipid mixtures outlined in Table I. This method of liposome preparation was chosen to reflect a more natural release process as opposed to a method involving addition of Aβ to preformed liposomes.

The release of Aβ occurs from plasma, endosomal, lysosomal, and Golgi membranes by proteolysis (12–14). All experiments were done at a pH of 7.4 to represent a physiological extracellular pH. However, to model whether or not the more acidic environment of the endosomal pathway is significant we have carried out a number of our experiments at a pH of 5.5. The common endosomal and lysosomal pH values are thought to be 6.0 and 4.5–5.5, respectively (15, 16); consequently we chose 5.5 to be representative of both organelles. We report here the mode of interaction of Aβ-(1–40) and a mixture of Aβ-(1–40)/Aβ-(1–42) (10/1) with each of the four types of liposome as revealed by CD, turbidity, and negative-stained TEM measurements.

EXPERIMENTAL PROCEDURES

Lyophilized amorphous powders of synthetic Aβ-(1–40) and -(1–42) from dimethyl sulfoxide (Me_2SO) were obtained from Peptide Institute Inc. (Osaka, Japan). Purities were analyzed by HPLC and amino acid analyses. Egg yolk L-α-phosphatidylcholine (egg PC), egg yolk L-α-phosphatidylethanolamine (egg PE), bovine brain L-α-phosphatidyl-L-serine (PS), bovine brain galactocerebroside (Cer), bovine brain sphingomyelin (SM), and Ch were purchased from Sigma-Aldrich Japan K. K. (Tokyo). Bovine brain ganglioside GM1, 1,1,1,3,3,3-hexafluoro-2-propanol (HFIP), and other chemicals were purchased from Wako Pure Chemical Ind, Ltd. (Osaka, Japan).

It has been recognized that the self-assembly of Aβ is dependent on the initial Aβ structure, *i.e.* whether it is monomeric and has a random coil structure or whether it has a β-sheet structure (17, 18). In the present study, the lyophilized powders of the peptide(s) were dissolved in HFIP, a solvent well known for its good solubilizing and α-helical structure-promoting properties. In HFIP solution, Aβ is monomeric (19–21). The peptide stock solution was made by dissolving the lyophilized amorphous powder in HFIP. Each liposome, composed of the appropriate mixture of lipids and peptide, was prepared by hydration and sonication of a film obtained from the evaporation of a mixture of the lipids in $CHCl_3$ solution and Aβ in HFIP solution.

CD Spectrum Measurements—Mixed films of lipids and Aβ-(1–40) or Aβ-(1–40)/Aβ-(1–42) (10/1) in HFIP were prepared by evaporating the organic solvents under a stream of nitrogen. Any residual solvent in the film was removed *in vacuo* overnight. Films were hydrated in Tris buffer solution (5 mM Tris, 100 mM NaCl, pH of 7.4 or 5.5) and sonicated by ultrasonic irradiation in the cuphorn of a Branson Model 185 sonifier (Danbury, CT). Solutions were sonicated at room temperature for about 30 min until they became transparent. CD spectra were measured on a JASCO J-600 apparatus (JASCO, Tokyo, Japan) controlled by a personal computer (NEC PC-9801) using a 1-mm pathlength quartz cell at 25 °C. Four scans were averaged for each sample. An averaged blank spectrum (vesicle suspension or solvent) was subtracted from each sample spectrum. The peptide and lipid concentrations were 50 μM and 1 mM, respectively. Conformational analyses were performed using CONTIN3 in a software package for analyzing protein CD spectra (CDPro) via the Internet (22). In our experiments, the program has been successfully applied to the solutions of peptides consisting of α-helix, β-sheet structure, β-turn, and random structure such as the p53 tetramerization domains that have been well characterized by NMR (23).

Turbidity Measurements—A mixed solution of lipids in chloroform and Aβ in HFIP measured to the appropriate peptide/lipid mol ratio was placed in a round bottom flask and dried under a stream of N_2 gas. The residual films were further dried overnight *in vacuo* and then hydrated with Tris buffer saline solution (5 mM Tris, 100 mM NaCl, pH of 7.4 or 5.5) by vortexing and then sonicated as described above. Lipid concentrations were kept to a concentration of 100 μM in the same Tris buffer at 25 °C. The absorbance of the sample solution was recorded at 400 nm using a JASCO spectrometer (JASCO Corp., Tokyo, Japan) after vigorous vortexing.

Transmission Electron Microscopy (TEM)—Each sample was absorbed onto a carbon-coated copper grid (mesh) by floating a drop of sample solution. Excess solution was removed by filter paper blotting, the grid was washed by floating a drop of water, and then the water was removed. The sample on the grid was then negatively stained with an aqueous phosphotungstic acid (1.0%), and the excess staining solution was removed. After drying, the samples were imaged with a HITACHI HU-12A electron microscope (Hitachi, Japan) operating at 100 kV. Samples prepared for the CD experiments were also used for the TEM experiments. The peptide and lipid concentrations were 50 μM and 1 mM, respectively.

RESULTS

Compositions of Lipid Mixtures Similar to Cerebral Cortex Membrane—To investigate the roles of GM1 and Ch in Aβ-lipid interactions, we chose to model cerebral cortex membranes, because this is the main location of amyloid in the body. Values for the composition of total lipid extract from cerebral cortex membranes were those reported by Rossiter (24). Because of its easily oxidative property and its instability under acidic conditions, plasmalogen was not included in the model liposomes of this study. In the human cerebral cortex tissue, there is about 10% (w/w) of plasmalogen. We have adjusted the proportion of the other components to allow for this omission as shown in Table I, where we list the compositions of the four types of liposomes examined. Ch (26 mol %) is significantly more abundant in CCM membranes than GM1 (4 mol %).

Secondary Structure of Aβ-(1–40) in Lipid Bilayers—Amyloidogenesis involves a transition from random or α-helical to a β-structure, which is necessary for fibril formation *in vivo*. Thus we monitored the conformational change of Aβ-(1–40) or Aβ-(1–40)/-(1–42) (10:1, molar ratio) in the four liposome systems (Table I) by CD spectroscopy over a period of 7 days. In buffer solution, the peptide Aβ-(1–40) adopts a mainly random coil structure upon addition of the peptide stock solution to the buffer solution (Fig. 1*A*). This result agrees with the CD data reported previously (7, 25). Then, after 5 days, it takes a mainly β-sheet structure as suggested by the peak minimum around 218 nm. A conformational analysis of its spectrum showed 15% α-helix and 30% β-structure. This main structure still persisted after 7 days.

In the CCM membrane at pH 7.4 (Fig. 1, *B-a*), upon preparation from the lipid-peptide film, Aβ-(1–40) adopts a mainly random structure within the liposomes, however, after 1 day a

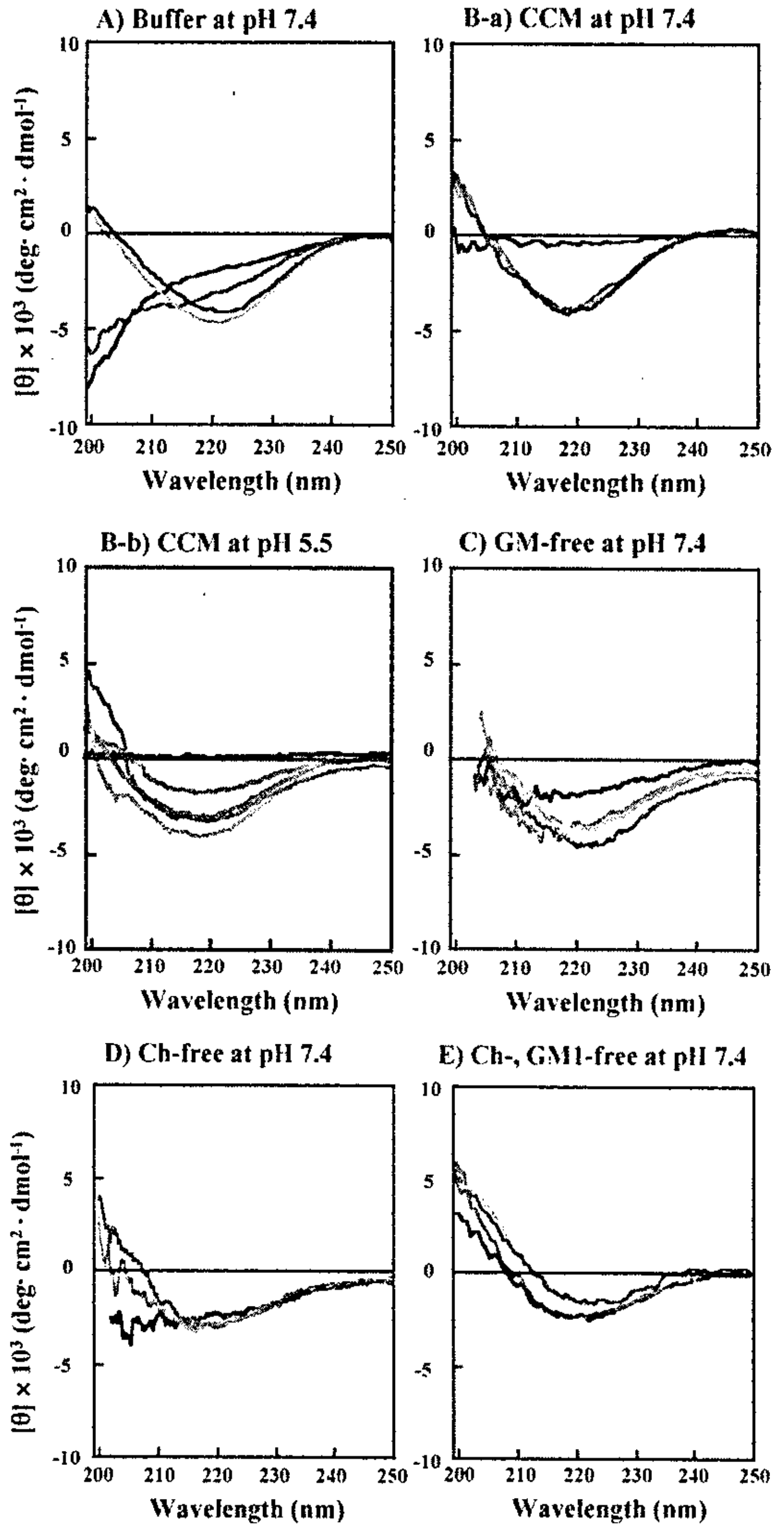

FIG. 1. **CD spectra of Aβ-(1–40) in Tris buffer (*A*), CCM at (*a*) pH 7.4 and (*b*) pH 5.5 (*B*), GM1-free (*C*), Ch-free (*D*), and Ch-GM1-free (*E*) liposomes.** Lipids over a period of 7 days after the incubation of peptides to liposomes are shown: immediately after preparation (*black*), at 1 day (*green*), 3 days (*red*), 5 days (*orange*), and 7 days (*blue*). Peptide and lipid concentrations are 50 and 1 μM, respectively.

broad negative band is seen around 218 nm, the intensity of which is approximately equal to that of the peak observed for the 7-day-old sample in buffer. But conformational analysis of the spectrum showed 60% β-structure and the same spectral pattern after 3, 5, and 7 days. When compared with the CD spectra in buffer, the β-structure formation was accelerated and more extensive. At pH 5.5, similar CD curves were obtained, though the rate of β-structure formation was significantly reduced. After 1 day under acidic conditions there was only 36% β-structure as compared with 60% at pH 7.4 (Fig. 1, *B-b*). On the other hand, the peptide in GM1-free lipid liposomes at pH 7.4 (Fig. 1*C*), showed a shallow negative band around 210 nm with 25% α-helix and 10% β-structure, and after 1, 3, and 5 days the negative band had shifted to 216 nm, corresponding to 45% β-structure and 10% α-helix, indicating that the absence of ganglioside slightly reduces formation of β-structure, compared with CCM membranes. Interestingly, in Ch-free membrane (Fig. 1*D*), Aβ-(1–40) had a negative band around 205 nm similar to that of GM1-free liposomes after preparation. Some α-helical structure (about 15%) was seen, but in time the band around 205 nm intensified, and a crossing point on the horizontal axis occurred characteristic of β-struc-

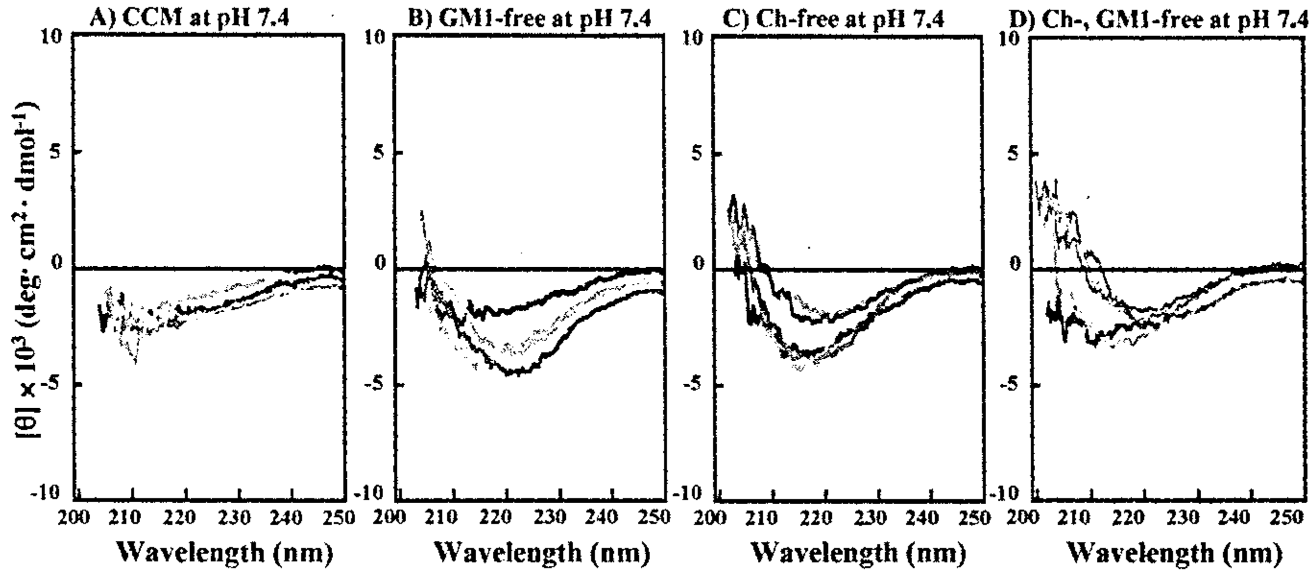

Fig. 2. **CD spectra of Aβ-(1–40)/Aβ-(1–42)(10/1) in CCM (*A*), GM1-free (*B*), Ch-free (*C*), Ch-GM1-free (*D*) over a period of 7 days after the incubation of peptides to liposomes.** Shown are spectra immediately after preparation (*black*), at 1 day (*green*), 3 days (*red*), 5 days (*orange*), and 7 days (*blue*). Peptide and lipid concentrations are 50 μM and 1 mM, respectively.

ture. After 3 days, β-structural content reached 50%, indicating, that in time, the absence of either Ch or the absence of GM1 led to a decrease in β-structure formation. For Ch- and GM1-free liposomes (Fig. 1*E*) at pH 7.4, Aβ-(1–40) showed a broad negative band around 220 nm upon preparation, there was some α-helical structure present. However, in time, the band shifted to 203 nm and became shallower, also the crossing point of the horizontal axis red-shifted to more than 210 nm, indicating decreased β-structure. In fact, the spectra could not be analyzed using the CDPro software (22). Similar CD spectra have been reported in which the spectrum has an atypical minimum at 223 nm and a maximum at 203 nm; this pattern is characteristic of amyloid fibers (26, 27). However, electron microscopy of Aβ-(1–40) did not detect any fibril structure in Ch-free or Ch-GM1-free membranes. These results indicated that the CD spectral patterns having the minimum at 223 nm and the maximum at 203 nm do not necessarily exhibit the characteristics of amyloid fibers. At pH 5.5, although the minima around 220 were shallower than those at pH 7.4, very similar CD curves were observed, and the fibril structure was not detected by TEM at either pH (data not shown). Consequently, it would appear that the presence of Ch and GM1 ganglioside is necessary for β-amyloid formation to occur.

CD Spectra of Aβ-(1–40)/Aβ-(1–42) (10:1)) in Lipid Bilayers—To investigate a seeding hypothesis in which aggregates of Aβ-(1–42) act as an initiation factor for early plaque formation, we examined changes in conformation of Aβ-(1–40)/-(1–42) (10:1, molar ratio) in the four model liposomes at pH 7.4 (Fig. 2) by circular dichroism spectroscopy. Our results show that in the CCM and Ch-free membranes, the rate of β-structure formation is greater than that for the corresponding Aβ-(1–40) liposomes. In CCM-lipid, upon preparation, we observed 40% β-structure which, after 1 day became 50%; for Aβ-(1–40) these values are 18 and 60% β-structure, respectively (Figs. 2*A* and 1*B*). In the GM1-free membrane, the CD spectral pattern of Aβ-(1–40)/-(1–42) is not different from that of Aβ-(1–40) (Figs. 2*B* and 1*C*). In Ch-free lipids, a mixture of Aβ-(1–40)/-(1–42) formed a β-structure more easily than the Aβ-(1–40) liposomes (Figs. 2*C* and 1*D*). Interestingly, in the Ch-GM1-free lipid liposomes upon preparation the peptide had a 35% β-structure and 10% α-helical structure. This was not observed for Aβ-(1–40) and in time it transformed the conformations to the other conformational mixture containing β-structure as described above (Fig. 2*D*). These results indicate that the rate of formation of the β-structure is generally promoted by the addition of Aβ-(1–40), although ultimately formation depends on lipid composition.

Turbidity Measurements—To monitor the aggregation or precipitation produced by lipid-peptide interactions, we measured the changes in turbidity in the buffer solution and solutions of the four Aβ-lipid mixture liposomes over a 7-day period (Fig. 3). Solution absorbance measured at 400 nm was plotted as a function of time. Days after successive film preparation, hydration, and sonication of mixture solutions for different ratios of Aβ-(1–40) and lipids are shown on the abscissa. The lipid concentration was kept at 100 μM. In the absence of liposomes, at a peptide concentration of 40 μM at pH 7.4, the absorbance gradually increased from 1 day and reached a maximum at 3 days, and then leveled out as a plateau (Fig. 3*A*). However, at lower peptide concentrations (5–20 μM), the aggregation behavior was dependent on peptide concentration. In conjunction with the CD results, it was concluded that increasing turbidity was attributable to β-structure formation, associated with Aβ aggregation.

For 40 μM Aβ in CCM liposomes at pH 7.4, solution turbidity gradually increased over 4 days, then it slightly decreased, but at lower peptide concentrations there was little change in turbidity (Fig. 3*B*). With the results of CD and TEM experiments in mind, little or no change in turbidity is due to an aggregation of Aβ-(1–40) to form a β-structure. Similar turbidity changes in CCM were obtained at pH 5.5 (date not shown). In the GM1-free liposomes at pH 7.4, solution turbidity did not change at the examined Aβ concentrations except for 40 μM peptide, where a slight decrease occurred 1 day after preparation and was followed by a gradual increase (Fig. 3*C*). Little or no change in turbidity was consistent with the CD and TEM results, which showed the formation of aggregated peptide-lipids particles (to be described below). Interestingly, in Ch-GM1-free lipid liposomes at pH 7.4, turbidities for 20 and 40 μM peptide decreased. For 40 μM peptide an especially dramatic decrease in turbidity occurred over the first day (Fig. 3, *E-a*). Similar changes in turbidity were observed at pH 5.5 (Fig. 3,

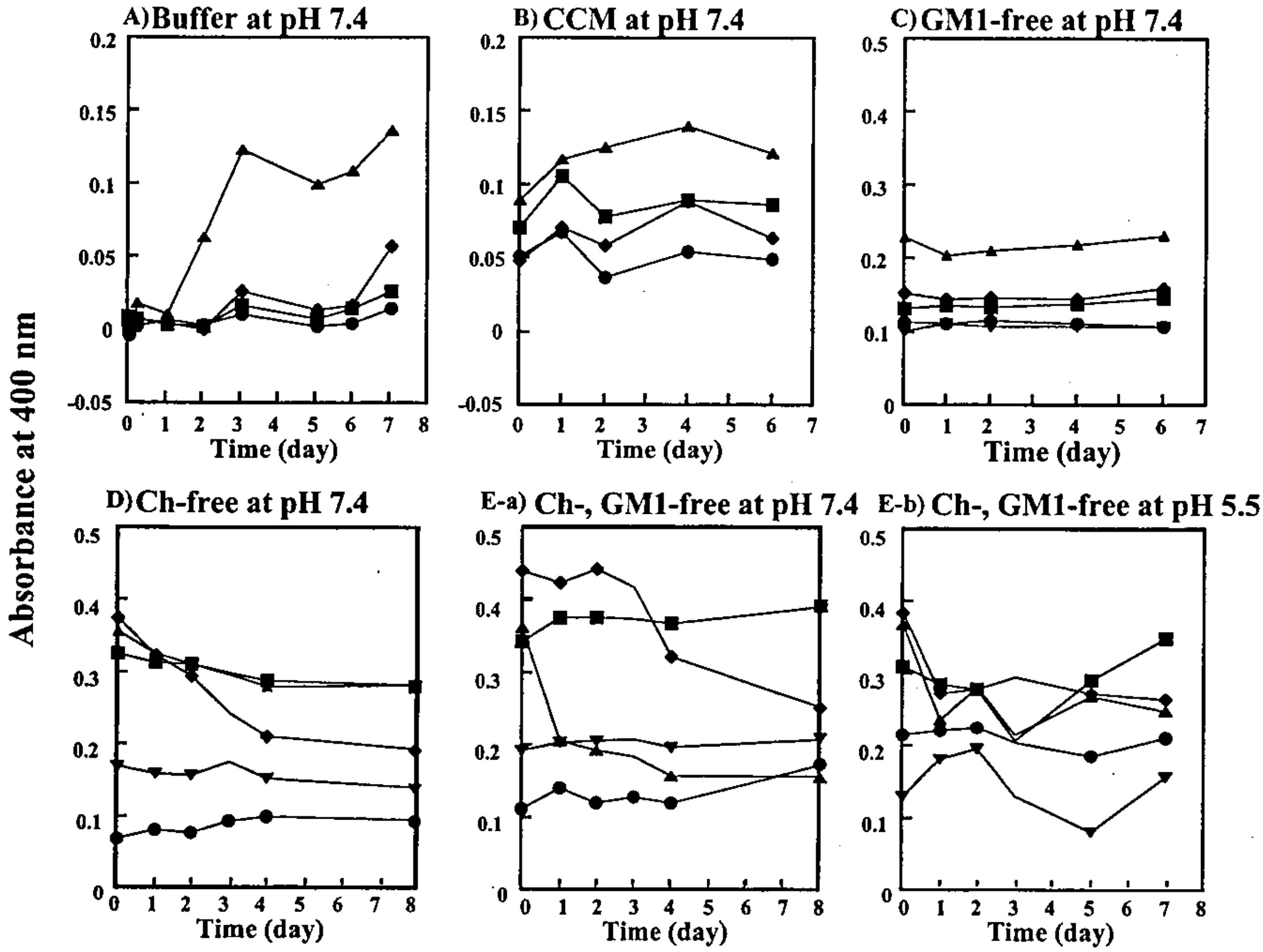

FIG. 3. **Changes in turbidity in buffer solution (*A*), CCM (*B*), GM1-free (*C*), Ch-free (*D*), Ch-GM1-free (*E*) at (*a*) pH 7.4 and at (*b*) pH 5.5 over a period of 7–8 days after the incubation of Aβ-(1–40) to liposomes.** Peptide concentrations are: 0 μM (●); 5 μM (▼); 10 μM (■); 20 μM (♦); and 40 μM (▲).

E-b). The decrease in turbidity indicated liposomes were solubilized by Aβ-(1–40), to form small peptide-lipid particles. The TEM image for this solution showed the liposomes became smaller with time and showed no fibril structure. Although a similar decrease in turbidity was observed for the Ch-free liposome solution (Fig. 3*D*), this was independent of peptide concentration; the turbidity of 20 μM Aβ was much larger than that of 40 μM. This also indicated that liposomes were solubilized and led to the formation of small particles.

Turbidity of Aβ-(1–40)/Aβ-(1–42) (10:1) was measured in CCM lipid and ChGM1-free lipid at pH 7.4 (data not shown). Initial turbidity did not depend on peptide concentration and did not change dramatically with time, which indicated the membrane solubilization did not occur as it did for Aβ-(1–40) in Ch-free and Ch-GM1-free membranes.

Studies by Transmission Electron Microscopy—To observe changes with time in the morphological characteristics of Aβ-(1–40) and Aβ-(1–40)/Aβ-(1–42) (10:1) both in buffer and in the liposomes we made measurements by TEM. Liposomes were prepared from a mixture of lipids (1 mM) and peptide (50 μM) and then examined over a period of 1–10 days under the electron microscope. The TEM samples were negatively stained. For Aβ-(1–40), after 1 day in buffer solution at pH 7.4, an indistinct fibril structure was observed, which after 10 days became better defined (Fig. 4*A*). In CCM lipid membrane at pH 7.4, a distinct fibril structure was observed, with a dark phospholipid membrane-like shadow after 1 day (Fig. 4*B-a, i*). After 10 days the same clear fibril structure seen in saline buffer was observed (Fig 4*B-a, iii*). At pH 5.5, lots of short filaments were visible after 1 day and clear long fibrils were observed after 3 days, indicating that the growth of fibril structure is slower than that at pH 7.4 (Fig 4*B-b*). This is consistent with the slower rate of β-structure formation seen by CD after 1 day at pH 5.5 relative to that at pH 7.4. In GM1-free membranes (Fig. 4*C*) at pH 7.4 after 1 day, long fibril structures were present along the surface of vesicles, which were probably large aggregated/fused liposomes. After 3 days, small vesicles emerged around the large aggregate liposomes, also some fibrils were still apparent along their surface. After 10 days we observed aggregates of small vesicles (several ten-fold nanometers in diameter). These results indicate that Aβ can disrupt the large liposomes into smaller vesicles, presumably by the formation of lipid-peptide complexes. After 1 day in the Ch-free membrane (Fig. 4*D*) at pH 7.4, a few relatively long fibrils were observed around the large liposomes. After 4 days, numerous small filament-like structures, probably lipid-peptide complexes, were present around the liposomes. Interestingly, after 10 days, thicker and longer fibrils (several ten-fold nanometers in diameter) were observed around the liposomes, which were different from the fibril structure observed in the buffer and CCM liposomes.

These results indicate that although the Ch-free membrane first releases some Aβ to create fibrils, in time, the membranes were slowly solubilized by Aβ to make short and thin fibrils and

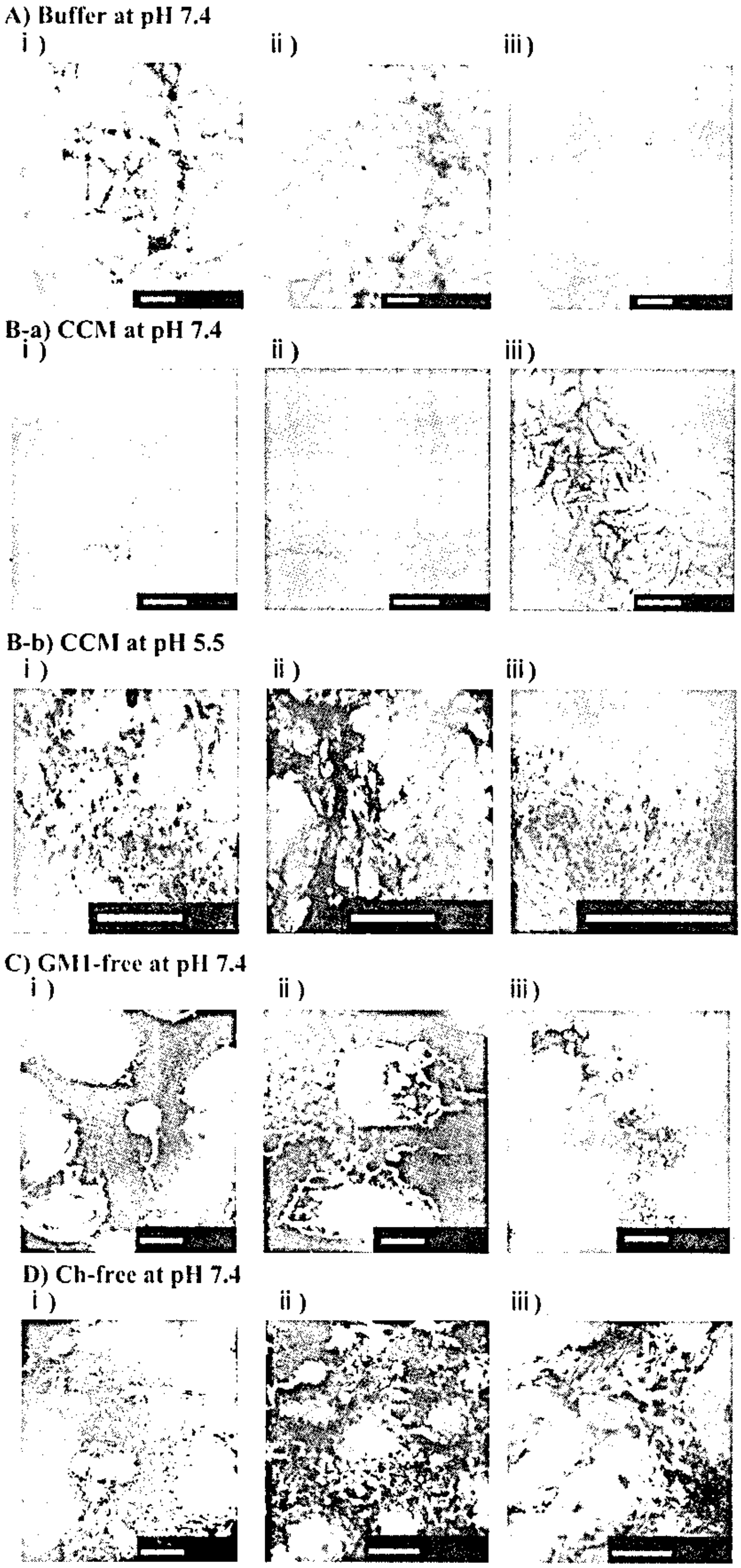

FIG. 4. **Electron micrographs in buffer solution (*A*), CCM at (*a*) pH 7.4 and at (*b*) pH 5.5 (*B*), GM1-free (*C*), Ch-free (*D*), Ch-GM1-free (*E*) at (*a*) pH 7.4 and at (*b*) pH 5.5 over a period of 14 days after the incubation of Aβ-(1–40) and in CCM (*F*) and Ch-GM1-free liposomes (*G*) of Aβ-(1–40)/Aβ-(1–42)(10:1).** Images: 1 day (i), 3 days (ii), 10 days (iii) after liposomes were prepared from 50 μM peptide and 1 mM lipid solutions, respectively. Bars are 500 nm.

eventually thicker and longer fibers. In Ch-GM1-free membranes at pH 7.4 and 5.5 (Fig. 4, *E-a* and *-b*) fibrils were not observed, liposomes of various shapes and sizes were present, and with time an increase in the number of smaller vesicles occurred.

Images of Aβ-(1–40)/Aβ-(1–42) (10:1) in CCM (Fig. 4*F*) were very similar to those for Aβ-(1–40) (Fig. 4*B*), showing indistinct fibril structures after 1 day and extensive well defined ones after 10 days (Fig. 4*F*). Similar images (not shown) were observed for GM1-free membranes. Interestingly, in Ch-GM1-

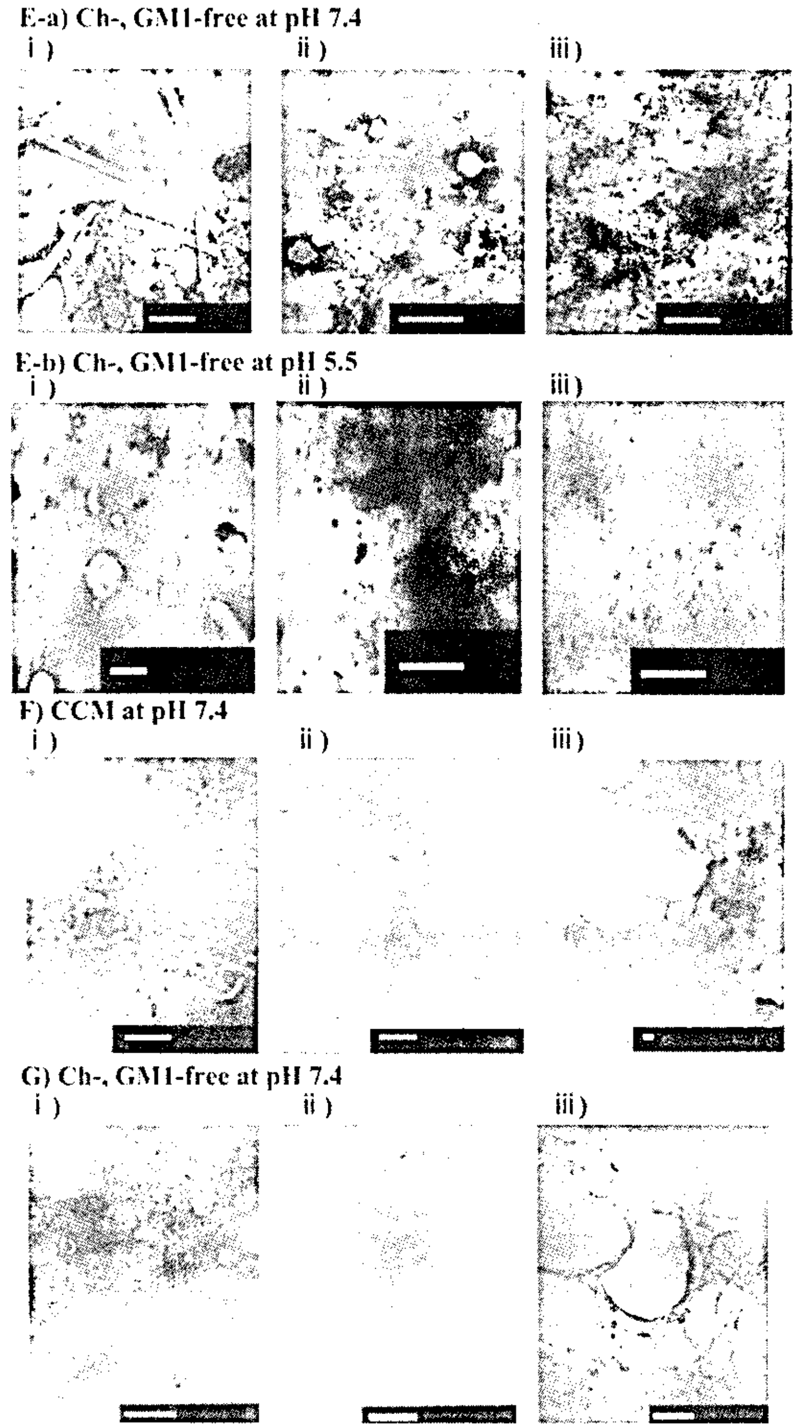

FIG. 4—*continued*

free membranes, both fibrils and spherical liposomes were present after 1 day, although with time the number of fibrils increased and the spherical liposomes disappeared (Fig 4*G*). Similar images (data not shown) were observed for the Ch-free membranes.

DISCUSSION

Because Aβ peptides are generated by the partial processing of the transmembrane α-helix of APP anchored in the brain membrane, their release from the membrane must play an important role in their subsequent aggregation and precipitation. Thus, to investigate how membrane lipids participate in the formation of fibril structure, we monitored the release of Aβ peptide from Aβ peptide-model membranes. Liposomes were prepared from Aβ and a lipid-mixture similar in composition to that of cerebral cortex membranes with and without ganglioside and/or cholesterol.

Our CD studies have shown that when a 50 μM solution of Aβ-(1–40) in HFIP solution is hydrated in buffer solution, it undergoes a transition from random coil to β-structure over a period of 3 days (Fig. 1*A*). This is consistent with the turbidity measurements. Over 24 h, the turbidity did not change, but it rapidly increased from 1 to 3 days, and only moderately after 3 days (Fig. 3*A*). From these results we propose that hydration of monomeric Aβ-(1–40) in organic solvent caused a slow change in conformation from random coil to β-structure. This β-structure then serves as a seed in the rapid formation of an extensive β-sheet structure (28). TEM measurements supported the presence of an extended fibril formation just 3 days after peptide hydration.

In CCM membranes at physiological pH (7.4), Aβ-(1–40) was mainly random coil after preparation, although some α-helical and β-sheet content was present (Fig. 1*B*). After 1 day, mainly β-structure had formed which persisted for 10 days. The turbidity increased moderately only for high concentrations of Aβ-(1–40) (Fig. 3*B-a*). TEM images of fibrals seen after 1 day (Fig. 4*B-a, i*) were clearer than those observed for the buffer solution. At pH 5.5 (Fig. 4*B-b, i*) the presence of fibrils after 1 day is uncertain, although after 3 days an extensive fibril formation is apparent (Fig. 4*B-b, ii*). For the CCM liposomes at endosomal pH the rate of formation of β-structure and fibrils is definitely slower than at physiological pH; however, the final resulting fibril structures appear the same. That Aβ fibril formation is pH-dependent has been reported in the literature (43).

From the CCM liposomes Aβ-(1–40) was released rapidly, and resulted in the formation of a fibril structure. In contrast, in GM1-free liposomes, Aβ-(1–40) consisted of a mixture of α-helix and β-structure and with time the proportion of β-structure increased. However, a slight increase in turbidity was observed for 40 μM Aβ. Its TEM image showed at first an incomplete short fibril structure around the lipid surface, and in time, small vesicles began to emerge, until finally only aggregates of small vesicles were visible (Fig. 4*C*). Apparently, Aβ was able to solubilize the ganglioside-deficient membrane into small vesicles.

In Ch-free Lipid liposomes, a similar change from α-helix to β-structure was observed. The turbidity decreased drastically for 20 μM Aβ, but not so for 40 μM. However, there were few signs of fibril structure after 1 day; instead spherical liposomes were visible (Fig. 4*D, i*). From 3 to 14 days, a gradual thickening and elongation of the thin, short fibrils around the spherical vesicles took place (Fig. 4, *D, ii* and *iii*). These fibrils were different in appearance to those observed in the buffer and CCM membranes. We propose these were peptide-phospholipid membrane complexes, because we have shown previously that highly hydrophobic peptides can form nanotubular fiber structures (29–31). Ch may assist in fibril formation, by promoting the release of Aβ-(1–40) from natural membranes. Interestingly, in both GM1- and Ch-free liposomes, the CD spectra show a shallow minimum around 223 nm (Fig. 1*D*), which was not seen for the CCM and GM1-free liposomes. Moreover, the TEM showed liposomes of various shapes and sizes, but no fibril structure was seen. These phenomena were the same at neutral and acidic pH membrane solutions. This suggests that the coexistence of Ch and ganglioside in the CCM membrane has a crucial role in the release of Aβ-(1–40) from the membrane and the subsequent formation of fibril structures.

A recent study has shown that in different lipid membranes Aβ can follow two pathways of assembly: pathway 1) the formation of fibril structure in the presence of acidic lipids; and pathway 2) the formation of small aggregates (but no fibril structures) in the presence of neutral lipids (32).

This study shows GM1-free membranes promote the formation of β-structure and small peptide-lipid vesicles, several ten-fold Angstrom in diameter. This process may take pathway 2; the absence of GM1 leads to the decrease in the acidity of the membranes, resulting in the elimination of Aβ-fibril formation. However, membrane disruption still occurs via the expansion of aggregated Aβ through the bilayers, resulting in the solubilization of membranes to form small peptide-lipid vesicles. Matsuzaki and Horikiri (33) reported that Aβ has a high affinity for GM1 ganglioside in the bilayer and is able to form a β-sheet structure. It has been reported that the tight binding of Aβ is to the sialic acid group of the GM1 (34). In the presence of GM1, Aβ probably follows pathway 1, a conformational transition from α-helix to a β-structure leading to fibril formation. However, tight binding of the peptide to GM1 may prevent its release from the membrane, resulting in accumulation of peptide and formation of a β-sheet scaffold structure. This may be the critical nucleus for fibril formation. After nucleation, fibril growth through the lipid bilayer results in destabilization of the membrane, leading to amyloid deposition or the formation of lipid particles (to be described below).

Ch promotes fibril structure formation as we observed by TEM; in the absence of Ch, a well defined fibril structure was not visible even after a few days. Interestingly, in the absence of Ch or GM1 Aβ does form a β-structure, so the formation of a β-structure does not necessarily lead to fibril formation. An increase in Ch in the membrane results in increased membrane stiffness and a decrease in membrane fluidity. Increased Ch content inhibits the insertion of Aβ into the membrane, resulting in an increase in Aβ concentration at the membrane surface and concomitant enhancement in the rate of Aβ fibrillogenesis (5). Therefore, the absence of Ch in the membrane will increase its fluidity, and so facilitate the insertion of the hydrophobic part of Aβ into the membrane (25). In Ch-free liposomes, the accumulation of Aβ into the membrane leads to its solubilization, resulting in the slow formation of thick fibril structures.

In the absence of both Ch and GM1, the characteristic CD pattern of β-structure with a negative at around 116 nm was not seen, and no fibril structure was observed by TEM. This suggests the coexistence of Ch and GM1 in the CCM membrane promote fibril formation. A strong decrease in turbidity at 40 μM Aβ was also observed. All of these results suggest that the Ch-GM1-free membrane was solubilized by Aβ (1–40). Yanagisawa *et al.* (6) have shown that GM1 ganglioside-bound amyloid β-proteins are a possible form of preamyloid in AD. They also reported that oligomeric Aβ can promote the release of lipid from neurons to form Aβ-lipid particles consisting of Ch, GM1, phospholipid, and Aβ. Recent model membrane studies using liposomes consisting of GM1, Ch, and sphingomyelin showed that an increase in GM1 as well as Ch changes the binding capacity of Aβ (7, 35). Our data indicate that GM1 and Ch strongly participate in the release of Aβ from the membrane and therefore are instrumental in amyloid precipitation.

It has been suggested that sphingolipids and cholesterol may exist as phase-separated "rafts" in sphingolipid and cholesterol-rich membranes such as the plasma membrane (36). The partial liquid-ordered rafts can be visualized as floating within the predominantly liquid crystalline "sea" of the lipid bilayer. Interestingly, it was proposed that the raft could be the site for the proteolytic processing of Alzheimer's amyloid precursor protein (APP) (37). Recently, we showed that elevating levels of sphingolipid and Ch cause decreased membrane fluidity and resulted in lipid-protein separations into liposomes containing α-helical transmembrane peptides (38). The proteolytic cleavage of APP to yield Aβ performed by both β-secretase and γ-secretase present in the raft may in fact involve the release of Aβ-lipid particles consisting of Ch, GM1, and phospholipid (8). However, in Ch- and GM1-free membranes, which are more fluid, Aβ is able to stay in the membrane, probably by insertion of its hydrophobic part into the lipid bilayer. The accumulation of Aβ in the membrane may result in its solubilization and eventual disruption into small vesicles.

The CCM consists of about 10% (w/w) plasmalogen (24), but the instability of this component under acidic conditions prevented its use in this study. We note, however, that it has been reported in the literature that levels of plasmalogen in AD CCM are reduced (39, 40).

Aβ-(1–42) has been recognized to be the more amyloidgenic component in plaques, since it has a greater propensity to form β-structure than Aβ-(1–40), a requirement for amyloid fibral formation. Consequently, aggregates of Aβ-(1–42) may act as an initiation factor for early plaque formation (10). In the present study, Aβ-(1–40)/-(1–42) (10:1, molar ratio) formed β-structure more readily than Aβ-(1–40) in all classes of liposome. Especially, in Ch-GM1-free membranes, where Aβ-(1–40) forms no β-structure, the mixture of Aβ-(1–40)/-(1–42) caused the gradual conversion of a predominantly α-helical structure into a mainly β-structure. Therefore, the presence of a small amount of Aβ-(1–42) can induce the formation of β-structure in Aβ-(1–40) and confirms the "seeding" hypothesis. Aβ-(1–42) is able to promote the formation of β-structure that accompanies the formation of fibrils.

Recent studies have demonstrated that amyloid plaque formation may be initiated in the plasma membrane and that deposits were associated with the extracellular leaflet of the plasma membrane (41, 42). Moreover, Aβ-amyloid peptides are generated from various intracellular compartments, including the endoplasmic reticulum, the Golgi apparatus, lysosomes, and endosomes. The present model studies are carried out at the extracellular and lysosomal/endosomal pH values of 7.4 and 5.5. The results for the CCM liposomes indicate a kinetic pH-dependence of fibril formation, but it is not clear whether the release of Aβ-(1–40) is also pH-dependent. The results seen for the Ch-GM1-free liposomes are the same in both pH environments; fibril formation does not occur. This definitely indicates that lipid bilayer composition plays an important role in the release of Aβ and might suggest that this release is much less dependent on the pH of the surrounding cytosol.

It has been shown that ganglioside and Ch participate in the mechanism of amyloid deposition in the presence of total brain lipid extract (5, 11, 34). However, until now there has been no report in the literature on the behavior of Aβ in membranes free of both Ch and GM1. We have shown that Ch and GM1 play an important role in the release of Aβ from liposome membranes designed to model cerebral cortex membranes, where fibril structure formation is known to be at its highest. In natural brain membranes, the Aβ generated from the processing of APP may be easily released from the membrane to play its correct biological role. However, the change of lipid composition in membranes by aging or other biological processes induces Aβ accumulation in membranes, this leads to formation of amyloid fibers or lipid-peptide particles, which are released into the cytosol, resulting in amyloid precipitation or cytotoxicity.

REFERENCES

1. Haass, C., Scholossmocher, M. G., Hung, A. Y., Vigo-Pelfrey, C., Mellon, A., Ostaszewski, B. L., Lieberburg, I., Koo, E. H., Schenk, D., Teplow, D. B., and Selkoe, D. J. (1992) *Nature* **359,** 322–325
2. Seubert, P., Vigo-Pelfrey, C., Esch, F., Lee, M., Dovey, H., Davis, D., Sinha, S., Schlossmacher, M. G., Whaley, J., Swindlehurst, C., McCormack, R., Wolfert, R., Selkoe, D. J., Lieberburg, I., and Schenk, D. (1992) *Nature* **359,** 325–327
3. Bunnell, W. L., Pham, H. V., and Glabe, C. G. (1998) *J. Biol. Chem.* **273,** 31947–31955
4. Waschuk, S. A., Elton E. A., Darabi, A. A., Fraser, P. E., and McLaurin, J. (2001) *J. Biol. Chem.* **276,** 33561–33568
5. Yip, C. M., Elton, E. A., Darabie, A. A., Morrison, M. R., and McLaurin, J. (2001) *J. Mol. Biol.* **311,** 723–734
6. Yanagisawa, K., Odaka, A., Suzuki, N., and Ihara, Y. (1995) *Nat. Med.* **1,** 1062–1066
7. Kakio, A., Nishimoto, S., Yanagisawa, K., Kozutsumi, Y., and Matsuzaki, K (2001) *J. Biol. Chem.* **276,** 24985–24990
8. Michikawa, M., Gong, J.-S., Fan, Q.-W., Sawamura, N., and Yanagisawa K. (2001) *J. Neurosci.* **21,** 7226–7235
9. Ueda, K., Fukui, Y., and Kageyama, H. (1994) *Brain Res.* **639,** 240–244
10. Jarrett, J. T., and Lansbury, P. T., Jr. (1993) *Cell* **73,** 1055–1058
11. Yip, C. M., Darabie, A. A., and McLaurin, J. (2002) *J. Mol. Biol.* **318,** 97–107
12. De Strooper, B., and Annaert, W. (2000) *J. Cell Sci.* **113,** 1857–1870
13. Mills, J., and Reiner, P. B. (1999) *J. Neurochem.* **72,** 443–460
14. Li, Y., Xu, C., and Schubert, D. (1999) *J. Neurochem.* **73,** 1477–1482
15. Moriyama, Y., Maeda, M., and Futai, M. (1992) *FEBS Lett.* **302,** 8–24
16. Cain, C. C. (1989) *Proc. Natl. Acad. Sci. U. S. A.* **86,** 544–568
17. Walsh, D. M., Lomakin, A., Benedek, G. B., Condron, M. M., and Teplow. D. B. (1997) *J. Biol. Chem.* **272,** 22364–22372
18. McLaurin, J., and Chakrabartty, A. (1996) *J. Biol. Chem.* **271,** 26482–26489
19. Barrow, C. J., Yasuda, A., Kenny, P. T., and Zagorski, M. G. (1992) *J. Mol. Biol.* **225,** 1075–1093
20. Shen, C. L., and Murphy, R. M. (1995) *Biophys. J.* **69,** 640–651
21. LeVine III, H. (2002) *Arch. Biochem. Biophys.* **404,** 106–115
22. Sreerama, N., and Woody, R. W. (2000) *Anal. Biochem.* **28,** 252–260
23. Jeffrey, P. D., Gorina, S., and Pavletich, N. P. (1995) *Science* **267,** 1498–1502
24. Rossiter, R. J. (1962) *Neurochemistry*, 2nd Ed., Charles C. Thomas, Springfield
25. Ji, S.-R., Wu, Y., and Sui, S.-F. (2002) *J. Biol. Chem.* **277,** 6273–6279
26. Huang, T. H. J., Yang, D.-S., Plaskos, N. P., Go, S., Yip, C. M., Fraser, P. E., and Chakrabartty, A. (2000) *J. Mol. Biol.* **297,** 73–87
27. Gorman P. M., Yip, C. M., Fraser, P. E., and Chakrabartty, A. (2003) *J. Mol. Biol.* **325,** 743–757
28. Burdick, D., Soreghan, B., Kwon, M., Kosmoski, J., Knauer, M., Henschen, A., Yates, J., Cotman, C., and Glabe, C. (1992) *J. Biol. Chem.* **267,** 546–554
29. Kitamura, A., Kiyota, T., Tomohiro, M., Umeda, A., Lee, S., and Sugihara, G. (1999) *Biophys. J.* **76,** 1457–1468
30. Lee, S., Furuya. T., Kiyota, T., Takami, N., Murata, K., Niidome, Y., Bredesen, D. R., Ellerby, H. M., and Sugihara, G. (2001) *J. Biol. Chem.* **267,** 41224–41229
31. Furuya, T., Kiyota, T., Lee, S., Inoue, T., Sugihara, G., Logvinova, A., Goldsmith, P., and Ellerby, H. M. (2003) *Biophys. J.* **84,** 1959–1959
32. Yip, C. M., and McLaurin, J. (2001) *Biophys. J.* **80,** 1359–1371
33. Matsuzaki, K., and Horikiri, C. (1999) *Biochemistry* **38,** 4137–4142
34. McLaurin, J., Franklin, T., Fraser, P. E., and Chakrabartty A. (1998) *J. Biol. Chem.* **273,** 4506–4515
35. Ferraretto, A., Pitto, M., Palestini, P., and Masserini, M. (1997) *Biochemistry* **36,** 9232–9236
36. Brown, D. A., and London, E. (1998) *Annu. Rev. Cell Dev. Biol.* **14,** 111–136
37. Lee, S. J., Liyanaga, U., Bickel, P. E., Xia, W., Lansbury, P. T., Jr., and Kosik, K. S. (1998) *Nat. Med.* **4,** 730–734
38. Shigematsu, D., Matsutani, M., Furuya, T., Kiyota, T., Lee, S., Sugihara, G., and Yamashita, S. (2002) *Biochim. Biophys. Acta* **1564,** 271–280
39. Ginsberg, L., Rafique, S., Xuereb, J. H., Rapoport, S. I., and Gershfeld, N. L. (1995) *Brain Res.* **698,** 223–226
40. Han, X., Holtzman, D. M., and McKeel, D. W., Jr. (2001) *J. Neurochem.* **77,** 1168–1180
41. Natte. R., Yamaguchi, H., Maat-Schieman, M, L. C., Prins, F. A., Neeskens, P., Roos, R. A. C., and van Duinen, S. G. (1999) *Acta Neuropathol.* **98,** 577–582
42. Torp, R., Head, E., Milgram, N. W., Hahn, F., Ottersen, O. P., and Cotman, C. W. (2000) *Neuroscience* **96,** 495–506
43. Esler, W. P., Stimson, E. R., Ghilardi, J. R., Vinters, H. V., Lee, J. P., Mantyh, P. W., and Maggio, J. E. (1996) *Biochemistry* **35,** 749–757

Available online at www.sciencedirect.com

SCIENCE DIRECT

Regulatory Peptides 120 (2004) 227–236

REGULATORY PEPTIDES

www.elsevier.com/locate/regpep

Eight-residue Aβ peptides inhibit the aggregation and enzymatic activity of Aβ42

Yoichi Matsunaga[a,*], Akihiro Fujii[b], Aradhana Awasthi[a], Junichi Yokotani[b], Tadakazu Takakura[b], Tatsuo Yamada[a]

[a] Fifth department of Internal Medicine, School of Medicine, Fukuoka University, 7-45-1, Nanakuma, Jonan, Fukuoka 814-0133, Japan
[b] Discovery Laboratories, Toyama Chemical Co. Ltd., Toyama, Japan

Received 10 January 2003; received in revised form 15 March 2004; accepted 16 March 2004

Available online 7 May 2004

Abstract

Insoluble Aβ1–42 is the main component of the amyloid plaque. We have previously demonstrated that exposure to low pH can confer the molten globule state on soluble Aβ1–42 in vitro [Biochem. J. 361 (2000) 547] and unfolding experiments with guadinine hydrochloride (GdnHCl) have now confirmed this observation. The molten globule state of the protein has many biological properties and understanding the mechanisms of its formation is an important step in devising a therapeutic strategy for Alzheimer's disease (AD). We therefore investigated the ability of a series of synthetic eight-residue peptides derived from Aβ1–42 to inhibit the acid-induced aggregation of Aβ1–42 and identified the potent peptides to be Aβ15–22, Aβ16–23 and Aβ17–24. A1-antichymotrypsin, a member of the serine proteinase inhibitor (serpin) family is another major component of the amyloid plaque. In the present study, we investigated the proteolytic activity of Aβ1–42 against casein at different pHs. Chemical modification of amino acid residues in Aβ1–42 indicated that serine and histidine residues, but not aspartic acid, are necessary for enzymatic activity, suggesting that it is a serine proteinase. Amino acid substitution studies indicate that glutamic acids at positions 11 and 22 participate indirectly in proteolysis and we surmise that amino acid residues 29–42 are required to stabilize the conformer. A study of metal ions suggested that Cu^{2+} affected the enzymatic activity, but Zn^{2+} and Fe^{2+} did not. Interestingly, Aβ14–21 and Aβ15–22 were the only peptides that inhibited the proteolytic activity of Aβ42. Therefore, Aβ15–22 may control both aggregation of Aβ1–42 at acidic pH and its proteolytic activity at neutral pH. Consequently, we suggest that it may be of use in the therapy of Alzheimer's disease.

Keywords: Alzheimer's disease; Serine-like proteinase activity; Proteinase inhibitor; Guadinine hydrochloride; Metal ions

1. Introduction

The deposition of amyloid plaque in the extracellular space, and neurofibrillary tangles in the neurons, are specific pathological features of Alzheimer's disease (AD) [1]. The main component of the amyloid plaque is insoluble Aβ1–42 (Aβ42), which adopts a structure rich in antiparallel β-pleated sheets. There have been many studies of the biological properties of Aβ42 such as self-aggregation [2], binding to other proteins such as apolipoprotein E [3], cytotoxicity for neuronal cells [4,5], vasoconstriction [6] and proteolytic activity against casein [7]. Recently, increasing awareness of amyloid beta protein (Aβ) intermediates as molten globule states has paralleled insight into the biological activities of the Aβ conformer [8,9]. The molten globule state of Aβ42 displays a less ordered, metastable conformation that is stabilized by the formation of fibrils [10,11]. Elucidation of the initial events causing aggregation and conversion of the soluble Aβ peptide into insoluble conformers, and other factors influencing the molten globule states of the Aβ conformer, are important aspects of a therapeutic strategy for AD.

Abbreviations: ELISA, enzyme-linked immunosorbent assay; AD, Alzheimer's disease; Aβ, amyloid beta protein; GdnHCl, guadinine hydrochloride; EDTA, ethylene diamine tetraacetate; DEPC, diethyl pyrocarbonate; PK, proteinase K; PMSF, phenylmethylsulfonyl fluoride; DFP, di-isopropylfluorophosphate; EPNP, 1,2-epoxy-3-(*p*-nitrophenoxy) propane.

* Corresponding author. Tel.: +81-92-801-1011; fax: +81-92-865-7900.
E-mail address: yoichima@fukuoka-u.ac.jp (Y. Matsunaga).

0167-0115/$ - see front matter © 2004 Elsevier B.V. All rights reserved.
doi:10.1016/j.regpep.2004.03.013

We have already demonstrated that the conformation of Aβ42 varies at different pHs, that the critical pH for the change is 4.6, and that the conformer has a different susceptibility to proteinase K within the environment of a glial cell [12]. We therefore suggested that lowering the pH might generate the molten globule state of soluble Aβ42 in vitro. In the present study, we have performed unfolding experiments with acid-treated Aβ42 intermediates, using guadinine hydrochloride, and have confirmed our previous results. It has been reported that the Aβ peptide exists either mainly as a random coil/α-helical structure or a β-sheet structure depending on pH [2], and that the kinetics of aggregation depend on which of these structures is involved, as well as on the length of the peptide examined [13,14]. The aggregation process is known to be driven by hydrophobic interactions [15]. Hence, the adoption of a structure rich in β-sheet at acidic pH accelerates the aggregation of Aβ, and the abnormal Aβ is stabilized by intermolecular interactions with other Aβ monomers that have the ability to form a β-sheet conformation [16].

We have synthesized a series of partial eight-residue peptides derived from Aβ42 to study their ability to inhibit acid-induced aggregation of Aβ42. The common feature of amyloidosis-related disorders is the abnormal folding of a natural protein into a pathologic conformer that is proteinase resistant [17]. We therefore also investigated the ability of the short peptides to reverse the proteinase K susceptibility of Aβ aggregates in glial cells. Our previous data indicated that epitopes around residues 9–14 and 17–21 in Aβ42 were dramatically affected by acidic pH [12] and our present results indicate that peptides in the vicinity of Aβ15–22, which contain the central hydrophobic region of Aβ42, are able to interfere with pH-induced Aβ42 aggregation. Small peptides of this kind may be useful for preventing the conformational changes leading to formation of Aβ intermediates in the early stages of Aβ aggregation.

Aβ has been shown recently to possess proteolytic activity against casein [7] and this novel activity may be implicated in the mechanisms of AD. It has also been reported that an A1-antichymotrypsin that belongs to the serine proteinase family of inhibitors (serpins) is a major additional component of the amyloid plaque [18,19]. The serum level of this inhibitor increases in response to the acute phase reaction of the host defence system [20,21]. It is mainly synthesized in the liver, although also produced by astrocytes [22], and may reduce the toxicity of the amyloid peptides in clonal cell lines as well as in cultures of primary cortical nerve cells by inhibiting their proteinase activity [23]. Thus, inhibition of the proteolytic activity of Aβ may be a useful approach for preventing cellular toxicity. In the present study, we investigated the proteolytic activity of Aβ42 and identified essential amino acid residues and further investigated effects of bioessential metal ions for the activity. We also investigated the ability of eight-residue peptides to inhibit proteolysis at neutral pH and found that short peptides around Aβ15–22 are effective.

2. Materials

2.1. Aβ peptides

Fig. 1 shows the synthetic partial-length Aβ peptides used in the present study: Aβ1–16, Aβ1–28, Aβ12–28, Aβ17–42, Aβ1–40 (Aβ40), Aβ1–42 (Aβ42) and two Aβ1–40 derivatives, namely Aβ40 (E11Q) and Aβ40 (E22Q) in which glutamic acid at either position 11 or 22 is replaced by glutamine. These were purchased from Anaspec (San Jose, CA). All Aβ peptides except for Aβ17–42 were dissolved in water at 1mg/ml. Aβ17–42 was dissolved in dimethyl sulfoxide (DMSO). Peptides were used at the indicated concentrations.

2.2. Chemicals

Rink Amide MBHA resin and all the protected amino acids were purchased from NovaBiochem (Switzerland). Bovine serum albumin (BSA), proteinase K (PK) and phenylmethylsulfonyl fluoride (PMSF) were from Boehringer Mannheim (Germany). Guadinine hydrochloride (GdnHCl), disodium hydrogen phosphate, citric acid, Tween-20, Tris[hydroxymethyl]-aminomethane and di-iso-

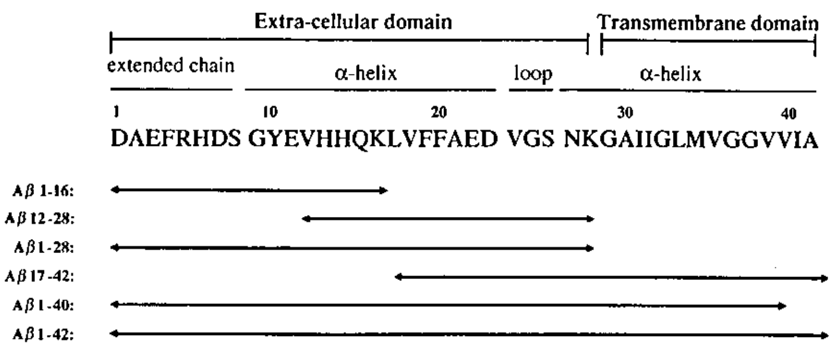

Fig. 1. Synthetic partial length Aβ peptides.